A structural epidemiological model for the optimal allocation of vaccines across countries

Manuel Huth*

July 17, 2021

Abstract

Description

Keywords: ...

---

*University of Bonn, e-mail: *s6mahuth@uni-bonn.de*

1 Introduction

... describe general SIR model, say that for biologists to remark compartmenst are different to biological compartments, thesis serves for both: epidemiologists inetrested in vaccine distribution but also for economcists or social scientists interested in compartment modleing

How it's currently done:

countries can decide to not take vaccine -> would be in our case assignment of zero vaccines

general model description: how do we deal with vaccines (most important), vaccination during infection, no vaccination during infection see here (US Center for Disease Control), no reinfections, no births and other deaths

The aim of a Stochastic Simulation algorithm (SSA) is to provide a computational model that allows for stochastic reactions. They can be classified as exact and approximate SSAs. Exact algorithms, like the Gillespie-Algorithm (Gillespie, 1977), do not group reactions together but model them one after another. Approximate algorithms, like $\tau-leaping$ (Gillespie, 2001), group reactions together and update the propensities within a larger interval τ. Thus, approximate algorithms might have an advantage when it comes to speed. However, by updating the propensities less often, we lose some accuracy.

2 Deterministic model

We subdivide the classic SIRD compartments, Susceptible (S), Infectious (I), Recovered (R) and Deceased (D), with sub-compartments allowing for heterogeneous areas of residence and vaccination states as well as infections by different virus types. Figure 1 illustrates the general model. Individuals either live in country A or country B. They are non-vaccinated U_0, vaccinated with vaccine one U_1 or vaccinated with vaccine two U_2. Vaccine U_1 represents the messenger ribonucleic acid (mRNA) vaccines and vaccine U_2 represent the vector vaccines. We assume that one vaccination shot is sufficient to get full protection of vaccine U_l. We introduce two virus types. A wild type W that serves as baseline variant and a more infectious mutant variant M.

To describe our model we denote every sub-group of individuals by a set $\mathcal{C}_t(F_n)$, where F_n is a placeholder for features that the individuals (elements) within the set $\mathcal{C}_t$ share and t denotes the time at which the set is evaluated. We illustrate the features F_n in the following with examples. Let X_i for $i \in \{S, I, R, D\}$ indicate to which general compartment an individual belongs, then, $\mathcal{C}_t(X_S)$ is the set of all susceptible individuals and $\mathcal{C}_t(X_I)$ is the set of all infectious individuals at t. If we want to distinguish not only between general compartments
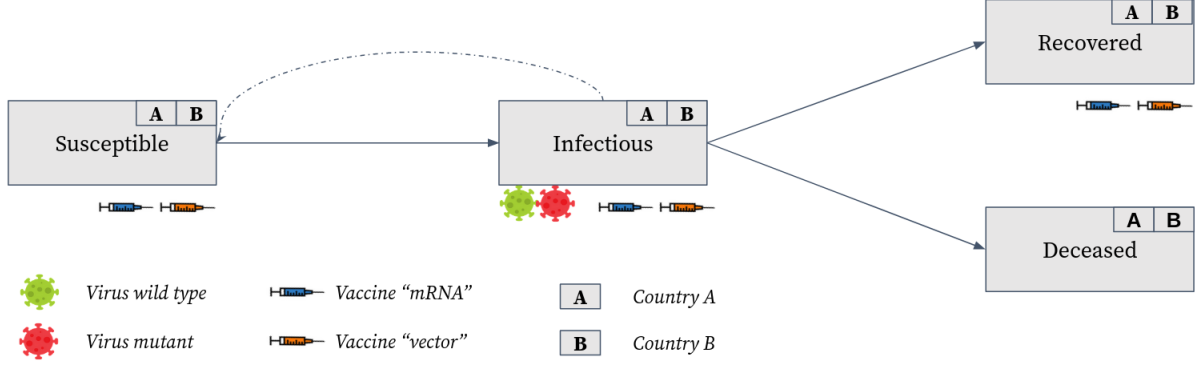
Note: Solid lines indicate transition paths and dashed lines indicate infections. Shots below a compartment indicate that individuals from this compartment are vaccinated. Viruses below a compartment indicate that this compartment is infectious. Each compartment is subdivided according to country of residence and vaccination status.

Figure 1: Model structure

but additionally between countries of residence, we use the feature C_j for $j \in \{A, B\}$ to indicate that the country of residence is j. $\mathcal{C}_t(X_S, C_A)$ is the set of all susceptible individuals of country A and $\mathcal{C}_t(X_S, C_B)$ of country B. Analogously, $\mathcal{C}_t(V_k)$ is the set of all individuals infected with virus k and $\mathcal{C}_t(U_l)$ is the set of all individuals with vaccination status l.

We can link sets with the common set operator, e.g. $\mathcal{C}_t(X_S, C_A) \cup \mathcal{C}_t(X_S, C_B) = \mathcal{C}_t(x_S)$ or $\mathcal{C}_t(X_S) \cap \mathcal{C}_t(X_I) = \emptyset$. The negation operator $\neg$ is used to indicate that a certain feature applies for all but the specified compartment, e.g. $\mathcal{C}_t(\neg X_D)$ is the set of all alive individuals. The cardinality $|\cdot|$ represents the respective number of individuals in a set, e.g. $|\mathcal{C}_t(X_S)|$ equals the number of all susceptible individuals. To shorthand notation, we define $y_t(F_n) = |\mathcal{C}_t(F_n)|$ as the number of individuals within the set $\mathcal{C}_t(F_n)$. By definition $\mathcal{C}_t() = \cup_{i \in \{S, I, R, D\}} \mathcal{C}_t(X_i)$ is the set of all individuals. An overview of all features is given in Table 1.

We impose a set of assumptions to the compartments to rule out undesired cases within the model

Assumption 1. *For all $t, r \in \mathbb{R}_+$, $k \in \{W, M\}$ and $s \in [-t, \infty)$ let*

$$\mathcal{C}_t(X_I, V_k) \cap \mathcal{C}_{t+r}(X_S) = \emptyset \tag{1.1}$$

$$\mathcal{C}_t(U_1) \cap \mathcal{C}_{t+s}(U_2) = \emptyset \tag{1.2}$$

$$\mathcal{C}_t(C_A) \cap \mathcal{C}_{t+s}(C_B) = \emptyset \tag{1.3}$$

$$\mathcal{C}_t(X_S, V_k) = \emptyset. \tag{1.4}$$

Assumption 1.1 rules out reinfections such that an individual that has been infected once cannot become reinfected after it had recovered. According to Roy (2020), there is evidence that recovered individuals cannot become reinfected but reinfections cannot be ruled out

Table 1: Notation

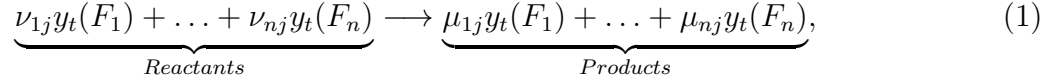| Feature	Code	Indices	Explanaition
General compartment	X_i	$i \in \{S, I, R, D\}$	Individuals can either be Susceptible (S), Infectious (I), Recovered (R) or Deceasesd (D).
Country of residence	C_j	$j \in \{A, B\}$	Individuals can either live in country A or B. We exclude cross-border movements.
Virus Type	V_k	$k \in \{W, M\}$	An infection can either be caused by the wild type (W) or the mutant (M) virus. This feature has to be understood, depending on X_i, as *is* or *has been* infected with type k.
Vaccine Type	U_l	$l \in \{0, 1, 2\}$	An individual can either be vaccinated with vaccine 1 or 2 or being unvaccinated (U_0).
Placeholder	F_n	$n \in \mathbb{N}$	A placeholder that is used to address an arbitrary combination of features. $\mathcal{C}_t(F_n)$ should be read as the set of a fixed but arbitrary compartment. If we need to distinguish between two arbitrary compartments, we use F_1 and F_2.

fully. However, the number of reinfected individuals might be negligible and we therefore do not incorporate reinfections to keep our model parsimonious. Assumption 1.2 implies that an individual only receives one type of vaccine. Receiving one vaccination shot in our model implies that an individual is fully protected according to the vaccine properties making it needless to assign a second shot to the same individual. Assumption 1.3 rules out permanent cross-country movements of individuals. We do so since permanent movements should not be a main driver of the pandemic and we therefore refrain from incorporating it to keep our model parsimonious. We incorporate cross-border infections by assigning a fraction of infections to be a cross-border infections. Assumption 1.4 ensures that susceptible individuals cannot be associated with any type of virus, since they have not been infected yet and can become infected with both virus types.

2.1 System of ordinary differential equations

We use a compartment SIRD model, based on a system of ordinary differential equations (ODEs), to simulate the pandemic. We see every subcompartment as own chemical species and each transmission, e.g. vaccinations, infections, recoveries, and deaths, as chemical reaction. Thus, our system becomes a chemical reaction network. To make this thesis self-contained, we explain how the dynamics of a chemical reaction network are modeled using ODEs. We can limit ourselves to the case of irreversible reactions since recovered and deceased individuals cannot become infectious again and infectious individuals become recovered but not susceptible.

Let $\mathcal{C}_t(F_1), \ldots, \mathcal{C}_t(F_n)$ be n pairwise disjoint sets and $\cup_{i=1}^n \mathcal{C}_t(F_i) = \mathcal{C}_t()$. Every irreversible

reaction R_j, for $j = 1, \ldots, m$, can be expressed as reaction of all compartments

$$\underbrace{\nu_{1j}y_t(F_1) + \ldots + \nu_{nj}y_t(F_n)}_{Reactants} \longrightarrow \underbrace{\mu_{1j}y_t(F_1) + \ldots + \mu_{nj}y_t(F_n)}_{Products}, \tag{1}$$

where $\nu_{ij} \in \mathbb{N}_0$ and $\mu_{ij} \in \mathbb{N}_0$ are called stoichiometric coefficients. If a compartment $\mathcal{C}_t(F_i)$ is not a reactant or product within reaction $,R_j$ the respective stoichiometric coefficients ν_{ij}, μ_{ij} are set to zero. ν_{ij} describes how much of species $\mathcal{C}_t(F_i)$ is consumed and μ_{ij} how much is produced within reaction R_j. The difference $\mu_{ij} - \nu_{ij}$ is the total change of $y_t(F_i)$ due to one reaction R_j.

We are not only interested in how one reaction (e.g. an infection, a vaccination, etc.) influences the state of the system but rather how often this happens within an interval $[t, t + \tau]$, for $\tau \in \mathbb{R}_+$. If we restrict us to the case $\tau = 1$, the latter is described according to the law of mass action by

$$v_j = r_j \prod_{i=1}^{n} y_t(F_i)^{\mu_{ij}}, \tag{2}$$

where r_j is a reaction specific constant. The product is the number of combinations to assign individuals from different compartments, that have $\mu_{ij} \neq 0$, together.

The change in the magnitude of $y_t(F_i)$ within the interval $[t, t + \tau]$ is given by the sum of the influences of all m reactions

$$y_{t+\tau}(F_i) - y_t(F_i) = \sum_{j=1}^{m} (\mu_{ij} - \nu_{ij})v_j\tau. \tag{3}$$

$(\mu_{ij} - \nu_{ij})$ is, as outlined above, the stoichiometry that specifies how one reaction influences the system, $v_j\tau$ is the number of times reaction R_j happens within the interval $[t, t + \tau]$, and therefore the product is the influence of R_j on $y_t(F_i)$ within $[t, t + \tau]$. Summed over all reactions yields the change of $y_t(F_i)$ within the system.

We divide both sides of (3) by τ, let $\tau \to 0$ and plug in (2) to obtain the ordinary differential equation

$$\dot{y}_t(F_i) = \sum_{j=1}^{m} \left[(\mu_{ij} - \nu_{ij})r_j \prod_{i=1}^{n} y_t(F_i)^{\mu_{ij}} \right]. \tag{4}$$

We write down the equations for all compartments in matrix form to obtain the system of

4

ODEs, which we use in subsequent chapters to ease notation.

$$\underbrace{\begin{pmatrix} \dot{y}_t(F_1) \\ \vdots \\ \dot{y}_t(F_n) \end{pmatrix}}_{Y(t)} = \underbrace{\begin{pmatrix} \mu_{11} - \nu_{11} & \cdots & \mu_{1m} - \nu_{1m} \\ \vdots & \vdots & \vdots \\ \mu_{n1} - \nu_{n1} & \cdots & \mu_{nm} - \nu_{nm} \end{pmatrix}}_{\mathbf{S}} \cdot \underbrace{\begin{pmatrix} v_1 \\ \vdots \\ v_m \end{pmatrix}}_{v} \tag{5}$$

Since our model consists of over 100 reactions, we do not write down the ODE system explicitly. However, it can be constructed as stated within this section.

2.2 Reactions

From a chemical point of view, our model can be divided into four major groups of reactions: 1. Infections, 2. Recoveries and Deaths and 3. Vaccinations. We group recoveries and deaths together, since their reactions have the same structure. We subsequently state the general and explicit reactions. We define the reactants, products, stoichiometric coefficients and reaction constants, such that that the ODE system (5) is determined. We emphasize reaction constants since they incorporate most information, such as vaccination status and infectiousness of the virus, of our model.
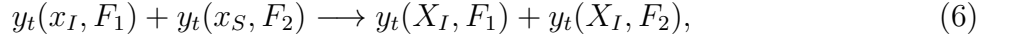
2.2.1 Infections
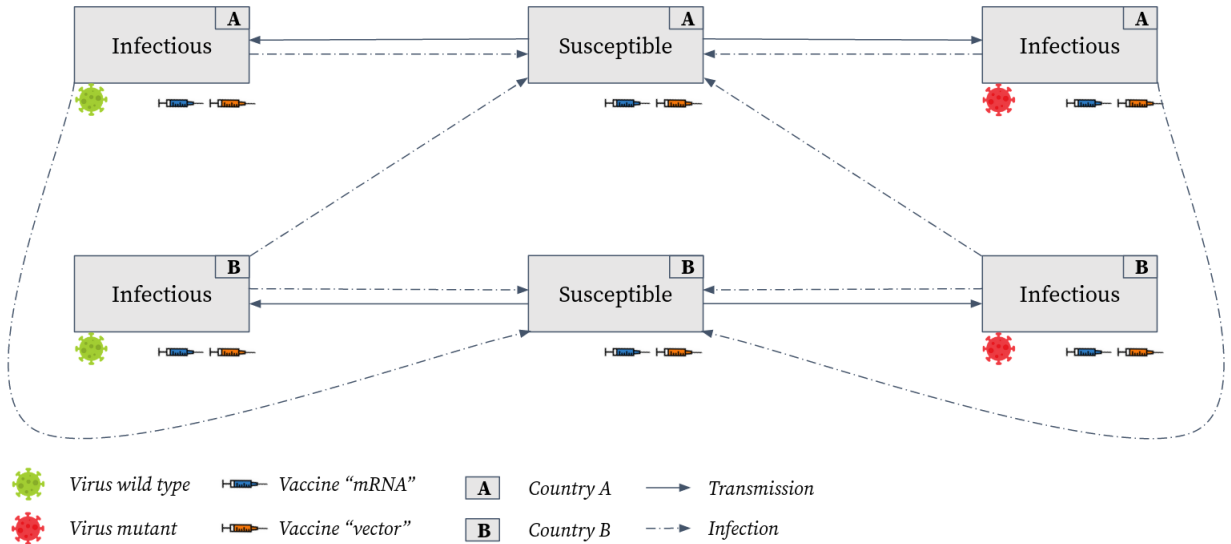
Note: Solid lines indicate transition paths and dashed lines indicate infections. Shots below a compartment indicate that individuals from this compartment can be vaccinated. Viruses below a compartment indicate that this compartment is infectious with the respective virus type. The letters in the top right corner of each compartment indicate the country of residence of individuals within the compartment.

Figure 2: Infection structure

Figure 2 depicts the structure of the transmissions from the susceptible to the infectious compartments. Every infectious individuals $i_1 \in \mathcal{C}_t(x_I)$ can infect a susceptible individual $i_2 \in \mathcal{C}_t(x_S)$ regardless of their countries of residence. However, we account for the higher chance of becoming infected due to an individual from the same country by shrinking the influence of the infectious compartments from the respective other country via the reaction constants.

In chemical terms, the compartments of two individuals i_1 and i_2 serve as reactants and their compartments with i_2 infected as products yielding the general form of the infection reactions

$$y_t(x_I, F_1) + y_t(x_S, F_2) \longrightarrow y_t(X_I, F_1) + y_t(X_I, F_2), \tag{6}$$

where we use F_1, F_2 to indicate that the reactions differ with respect to not explicitly mentioned features, e.g. vaccinated individuals have a lower risk of becoming infected or transmitting the virus, the mutant virus is more infectious, and cross-border infections are scaled by a factor to make them comparatively rare events. If $F_1 \neq F_2$, the stoichiometric coefficients are one. If $F_1 = F_2$, they are one for the reactants but two for the products while only having one product. We incorporate the additional features, represented by F_1 and F_2, within the reaction constants, which we label as *infection constants*

infection constant = infections per day × vaccine modifier × compartment adjustment

In the following, we elaborate on how to define the components of the *infections per day*, the *vaccine modifiers*, and the compartment adjustments.

Infections per day. To compute the infections per day we use the average number of contacts, between infectious and susceptible individuals, and multiply it with the proportion of individuals that become infected while meeting an infectious individual.

Let $c \in R_+$ be the average number of contacts per individual and day and $\alpha \in [0, 1]$ be the proportion of susceptible individuals that become infected if they meet a wild type infected individual without any vaccination of both individuals. Let $\eta \in (1, 1/\alpha]$ be the factor with which the mutant is more infectious than the wild type. Then $\beta = \alpha c$ is the average number of individuals infected per day by i_1 if $i_1 \in \mathcal{C}_t(X_I, V_w, U_0)$. If $i_1 \in \mathcal{C}_t(X_I, V_M, U_0)$ the average infected number increases to $\eta\beta$. We label β as *baseline infection constant*, since it covers the most basic case where the reaction happens between an unvaccinated susceptible individual and an unvaccinated wild type infected individual.

Vaccine modifier. Vaccinations influence the infections via two channels. First, vaccinated susceptible individuals are less likely to become infected, see Table 2 for a list references. Second, vaccinated infectious individuals are less likely to transmit the virus (Harris et al., 2021).

To account for the influence of the first channel, we introduce the parameters $\delta_{k,l} \in [0,1]$, where $k \in \{W, M\}$ indicates the virus type and $l \in \{1,2\}$ the vaccine type. $\delta_{k,l}$ is the reduce in the probability of becoming infected while meeting an infectious individual after being vaccinated. Thus, susceptible individuals are $1 - \delta_{k,l}$ times less likely to become infected while meeting an infectious individual. This is incorporated within the infection constant by multiplying the baseline infection constant with $1 - \delta_{k,l}$ if $i_s \in \mathcal{C}_t(X_S, U_1) \cup \mathcal{C}_t(X_I, U_2)$.

We account for the second channel two by introducing the parameter $\gamma \in [0,1]$. γ is the reduction in the probability of not transmitting the virus after being vaccinated, which we assume to be constant over time and across vaccines. Analogously to the first channel, we multiply the baseline infection constant with $(1-\gamma)$ if $i_1 \in \mathcal{C}_t(X_I, U_1) \cup \mathcal{C}_t(X_I, U_2)$.

Compartment adjustments. So far we have only defined the average number of contacts per day c of an infectious individual $i_1 \in \mathcal{C}_t(X_I, F_1)$ but not specified how these contacts are distributed across compartments. We use $\mathbb{P}_t(i_2 \in \mathcal{C}_t(X_S, C_j, F_2)|i_1 \in \mathcal{C}_t(X_I, F_1))$, the conditional probability that the second individual i_2 is susceptible and from compartment $\mathcal{C}_t(X_S, C_j, F_2)$, and multiply it by β to get baseline infection constant adjusted by the average number of contacts between i_1 and individuals of the compartment $\mathcal{C}_t(X_S, F_2)$. Note that the probability $\mathbb{P}_t$ depends on the state of the whole system $Y(t)$. To increase readability we omit conditioning on $Y(t)$ and directly define $\mathbb{P}_t$ to be conditioned on the state of the system $Y(t)$.

We assume that the vaccination status, the type of virus infection, and the exact general compartment (X_S, X_I, X_R) of i_1, are independent of $\mathbb{P}_t(i_2 \in \mathcal{C}_t(X_S, C_j, F_2))$. Thus, the problem facilitates to finding $\mathbb{P}_t(i_2 \in \mathcal{C}_t(X_S, F_2)|i_1 \in \mathcal{C}_t(\neg X_D, C_{j'}))$. This to say, the probability that the individual that can be infected (i_2) is susceptible, unvaccinated and from area two given that individual i_1 is infected with the wild type, unvaccinated and from area one. We facilitate our model and assume that the vaccination status as well as the type of virus infection of individual i_1 are independent of the features of i_2. Assuming independence of the vaccination status implies that an unvaccinated individual i_1 does not change her contact habits, given a certain number of meetings, compared to her counterfactual vaccinated self. Note that this does not mean that we assume that vaccinated and unvaccinated individuals have the same average number of contacts since the probabilities are defined on *conditioned a meeting occurs*. Differences in the average number of contacts between vaccinated and unvaccinated individuals can be incorporated implicitly via the vaccination parameter $\delta_{k,l}$.

To facilitate notation we subsequently take the perspective that the infectious individual

lives in country A. The same math applies vice versa. We provide a detailed derivation of the probabilities within the Appendix A.1.1.

$$\mathbb{P}_t(i_2 \in \mathcal{C}_t(X_S, C_j, F_2)|i_1 \in \mathcal{C}_t(\neg X_D, C_A)) = \begin{cases} 1 - \frac{y_t(X_S, C_j, F_2)}{y_t(\neg X_D)} \cdot b(d(A, B)), & j = A \\ \frac{y_t(X_S, C_j, F_2)}{y_t(\neg X_D)} \cdot b(d(A, B)), & j = B \end{cases} \quad (7)$$

The probability is in essence the relative population size adjusted for lower cross-border meeting frequencies by a penalty function $b : \mathbb{R}_+ \to [0, 1]$ that depends on the distances between both countries $d(A, B)$. By mapping the distance into the unit interval, we allow the probability of a cross-border meeting to be maximal as high as the relative population size. The distance can be interpreted as geographical distance but it could also serve to incorporate other factors, like favored holiday destinations, that encourage or discourage cross-border meetings. We impose three conditions on the function b

$$\lim_{b \to \infty} = 0 \qquad (B.1)$$

$$b(0) = 1 \qquad (B.2)$$

$$b(d_1) < b(d_2) \quad \text{if } d_1 > d_2. \qquad (B.3)$$

Condition $(B.1)$ ensures that countries that a very large distance only have small influences onto each other, $(B.2)$ defines a rather theoretical case where cross-border meetings are as likely as within-country meetings, and $(B.3)$ ensures that countries that have a greater distance have a smaller influence onto each other.

Explicit reactions. With the derived specifications of the infections per day, the vaccine modifiers, and the compartment adjustments, we are able to specify the compartment specific infection constants. We illustrate this by two examples.

Example 1. *Let the reactants be the compartments* $\mathcal{C}_t(X_I, C_A, V_W, U_0)$ *and* $\mathcal{C}_t(X_S, C_B, U_0)$. *The corresponding reaction is*

$$y_t(X_I, C_A, V_W, U_0) + y_t(X_S, C_B, U_0) \xrightarrow{r_{j_1}} y_t(X_I, C_A, V_W, U_0) + y_t(X_I, C_B, V_W, U_0), \quad (8)$$

where r_{j_1} *denotes the infection rate. To account for the infections per day, we use the baseline infection constant* β, *since the infectious compartment is infected with the wild type. The susceptible and the infectious compartments are unvaccinated. We therefore do not multiply by a vaccine modifier. However, the compartments are from different countries. We therefore*

adjust by multiplying with $\frac{y_t(X_S, C_j, F_2)}{y_t(\neg X_D)} \cdot b(d(A, B))$

$$r_{j_1} = \beta \cdot \frac{y_t(X_S, C_j, F_2)}{y_t(\neg X_D)} \cdot b(d(A, B)) \tag{9}$$

Example 2. *For the second example, we consider vaccinated and mutant infected compartments* $\mathcal{C}_t(X_I, C_A, V_M, U_1)$ *and* $\mathcal{C}_t(X_S, C_B, U_2)$ *as reactants to showcase the influence of the vaccine and the mutant modifier.*

$$y_t(X_I, C_A, V_M, U_1) + y_t(X_S, C_B, U_2) \xrightarrow{r_{j_2}} y_t(X_I, C_A, V_M, U_1) + y_t(X_I, C_B, V_M, U_2). \tag{10}$$

Since the infectious individual is infected with the mutant, we multiply the baseline infection constant with η*. Since the infectious compartment is vaccinated, we multiply the constant with* $(1 - \gamma)$*. Since the susceptible compartment is vaccinated with vaccine* U_2*, we multiply the infection constant with* $1 - \delta_M, 2$*. The compartments are from different countries. We therefore adjust by multiplying with* $\frac{y_t(X_S, C_j, F_2)}{y_t(\neg X_D)} \cdot b(d(A, B))$

$$r_{j_2} = (1 - \delta_{M,2})(1 - \gamma)\eta\beta\frac{y_t(X_S, C_j, F_2)}{y_t(\neg X_D)} \cdot b(d(A, B)). \tag{11}$$

To ensure readability we refrain from writing down all exact infections but they can be derived as shown in the two examples.
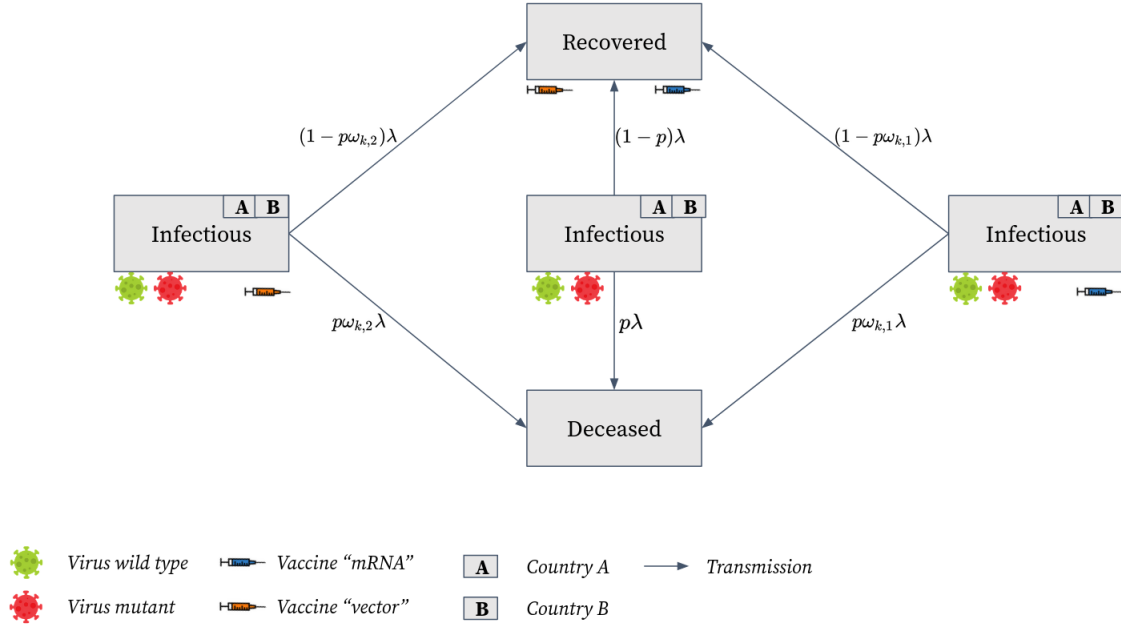
2.2.2 Recoveries and deaths

Figure 3 depicts the dynamics of the recoveries and deaths. The general reactions are defined by one infectious reactant and one product

$$\mathcal{C}_t(X_I, F_1) \longrightarrow \mathcal{C}_t(X_D, F_1) \tag{12}$$
$$\mathcal{C}_t(X_I, F_1) \longrightarrow \mathcal{C}_t(X_R, F_1).$$

The reaction number is the product of the average number of individuals transmitting out of the reactant compartment $\mathcal{C}_t(X_I, F_1)$ and the fraction of individuals that transmit to the product compartment, either $\mathcal{C}_t(X_D, F_1)$ or $\mathcal{C}_t(X_R, F_1)$.

Let $\lambda \in \mathbb{R}_+$ be the average number of individuals that transmit out of $\mathcal{C}_t(X_I, F_1)$. We assume that a constant fraction $p \in [0, 1]$ of these individuals dies. Hence, $p\lambda$ individuals transmit to the deceased and $(1-p)\lambda$ individuals transmit to the recovered state. The explicit

Figure 3: Structure of recoveries and deaths

reactions for unvaccinated individuals are for $i \in \{A, B\}$ and $k \in \{W, M\}$

$$\mathcal{C}_t(X_I, C_j, V_W, U_0) \xrightarrow{p\lambda} \mathcal{C}_t(X_D, C_j, V_w, U_0) \tag{13}$$
$$\mathcal{C}_t(X_I, C_j, V_w, U_0) \xrightarrow{(1-p)\lambda} \mathcal{C}_t(X_R, C_j, V_w, U_0)$$

$1/\lambda$ is the average durationan individual spends within $\mathcal{C}_t(X_I, F_1)$. We have implicitly assumed that this time is the same for deceasing and recovering individuals, which might not be accurate in real-world examples since deceasing individuals have more severe cases and heavier viral loads, such that they stay longer infectious. However, incorporating the seperated average duration would raise the need for more compartments. Since we allow for vaccinations of recovered and infectious individuals, we assume that this simplification is negligible. Moreover, note that p does not depend on the virus type. The virus type therefore only influences the number of infections but not the probability of dying for infected individuals. According to Davies et al. (2021) this assumption might be violated. We do so however, since we difference is rather low and we want to keep our model simple.

If the infectious individuals are vaccinated, they are less likely to decease (Tenforde, 2021; Voysey et al., 2021). To account for this reduce in the fraction that transmits to the deceased

state, we introduce the parameters $\omega_{k,l} \in [0,1]$, for $k \in \{W,M\}$ and $l \in \{1,2\}$. We use $p\omega_{k,l}$ as new probability of dying due to being infected with virus k after being vaccinated with vaccine l. $\omega_{k,l}$ is thus the reduction in the probability of dying. The corresponding reactions for vaccinated individuals are for $i \in \{A,B\}, k \in \{W,M\}$ and $l \in \{1,2\}$

$$\mathcal{C}_t(X_I, C_j, V_k, U_l) \xrightarrow{p\omega_{k,l}\lambda} \mathcal{C}_t(X_D, C_j, V_k, U_l) \tag{14}$$
$$\mathcal{C}_t(X_I, C_j, V_k, U_l) \xrightarrow{(1-p\omega_{k,l})\lambda} \mathcal{C}_t(X_R, C_j, V_k, U_l)$$

2.2.3 Vaccination
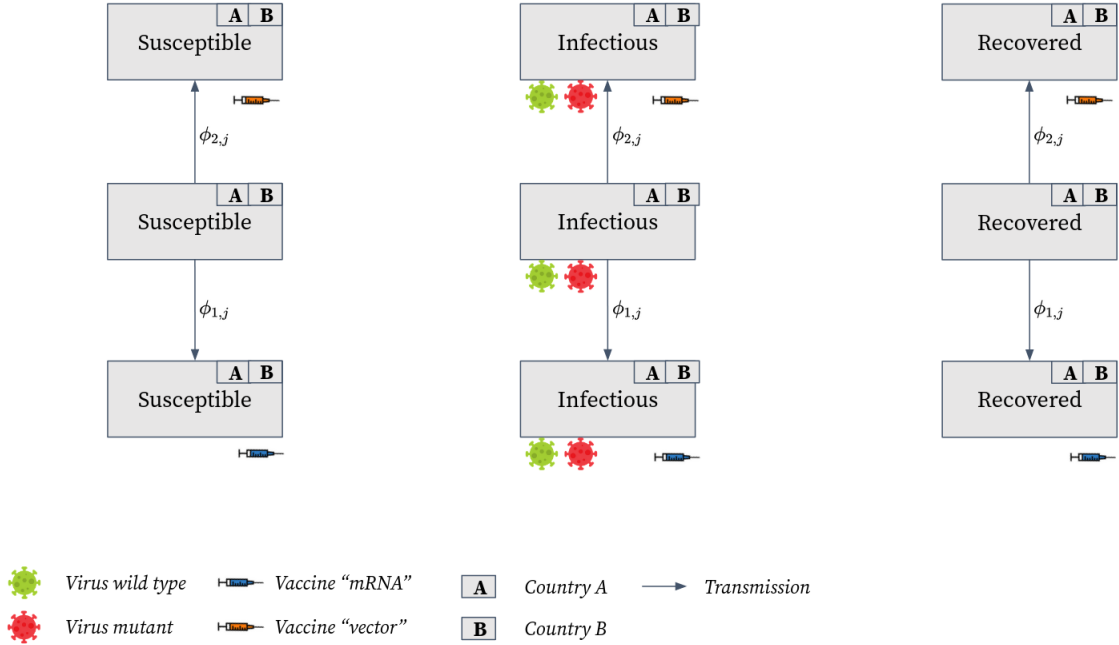
Note: Solid lines indicate transition paths. Shots below a compartment indicate that individuals from this compartment are vaccinated with the respective vaccine. Viruses below a compartment indicate that this compartment is infectious. The letters in the top right corner of each compartment indicate the country of residence of individuals within the compartment. The formulas next to the solid lines indicate the respective reaction constant.

Figure 4: Structure of vaccinations

Figure 4 depicts the vaccination dynamics. We allow for vaccinations of susceptible, recovered and, deceased individuals. We vaccinate susceptible individuals since these individuals to protect them from becoming infected. We vaccinate nfectious individuals to account for asymptomatic cases (Byambasuren et al., 2020) and recovered individuals to account to increase their degree of immunity (Skelly et al., 2021).

Let $\phi_{l,j} \in \mathbb{R}_+$ be the vaccination constant of vaccine l in country j at time t. The vaccination constant of one vaccine is assumed to be equal for all vaccination subcompartments

of S, I, R within one country, which is to say, that the decision of vaccinating an individual is independent whether it is susceptible, infectious or recovered. The corresponding reactions are for $j \in \{A, B\}$, $k \in \{W, M\}$ and $l \in \{1, 2\}$

$$\mathcal{C}_t(X_S, C_j, U_0) \xrightarrow{\phi_{l,j}} \mathcal{C}_t(X_S, C_j, U_l) \tag{15}$$

$$\mathcal{C}_t(X_I, C_j, V_k, U_0) \xrightarrow{\phi_{l,j}} \mathcal{C}_t(X_I, C_j, V_k, U_l)$$

$$\mathcal{C}_t(X_R, C_j, V_k, U_0) \xrightarrow{\phi_{l,j}} \mathcal{C}_t(X_R, C_j, V_k, U_l).$$

The vaccination constant is determined by the implemented vaccination policy. We explain how the vaccination constant is derived, given a vaccination policy, in Chapter 3.

3 Optimal vaccine allocation

The exercise to allocate vaccines across countries raises the need to specify the number of available vaccine shots. We see the number of available vaccines at any time t as exogenous and calibrate it based on the true number of COVID-19 vaccines that have been allocated to the EU.
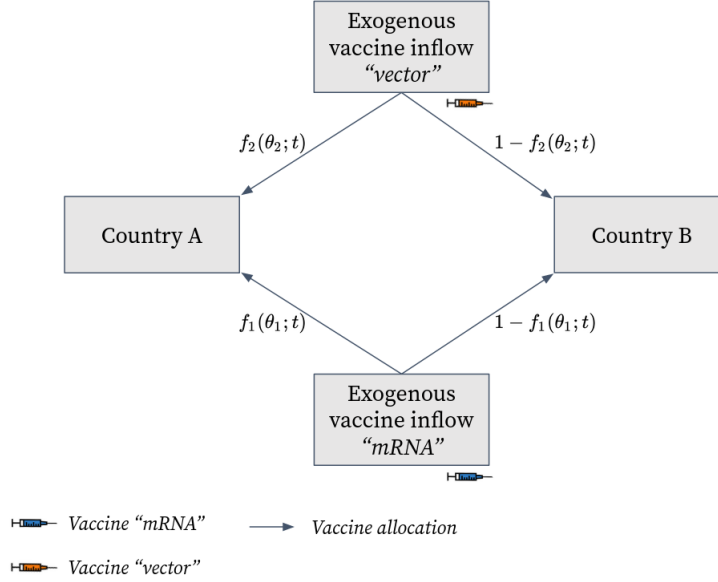
Note: Solid lines indicate vaccine allocations to a country. Shots below a box indicate the type of vaccines. The formulas next to the solid lines indicate the respective fractions of vaccines that are assigned to the country. The fractions depend on a parameter vector θ_l, over which we optimize to find the optimal solution.

Figure 5: Vaccine inflow and allocation across countries

Let $W_{l,j}(t)$ be the number of vaccination shots of vaccine l available at time t in country j and $W_l(t) = W_{l,A}(t) + W_{l,B}(t)$ be the the total number of available vaccine l shots at t. We

assume that all vaccine shots are vaccinated immediately.

Assumption 2. *The total number of vaccine l available in country j equals the number of vaccinated individuals for all $t \in [0, T]$.*

$$W_{l,j}(t) = \phi_{l,j} \cdot y_t(\neg X_D, C_j, U_0). \tag{16}$$

In the real-world, vaccinations take around 2 weeks to yield full protection (Centers for Disease Control and Prevention, 2021). With this regard, our model can be interpreted such that the number of lately vaccinated individuals is actually the number of individuals that lately received full protection by the vaccine. The vaccination constant would then be the constant defining the reaction of becoming protected.

At each point in time t, country A receives a fraction $f_l(\theta_l; t)$, with $f_l : \mathbb{R}^z \times [0, \tau] \to [0, 1]$, of vaccine W_l. The fraction depends on the time t and a parameter vector $\theta_l \in \mathbb{R}^z$ that parameterizes $f_l(\theta_l; t)$.

We assume that all vaccines stay within the two countries and no vaccines are wasted

Assumption 3. *The total number of vaccine shots of country j is equal to the number shots assigned to it*

$$W_{l,A}(t) = f_l(\theta_l; t)W_l(t) \tag{17}$$
$$W_{l,B}(t) = [1 - f_l(\theta_l; t)] W_l(t).$$

We use Assumption 2, Assumption 3, and solve for the vaccination constants. They depend on the vaccine inflow, the fraction of vaccine assigned to the respective country, and the total numbers of individuals that potentially can be vaccinated within the country

$$\phi_{l,A} = \frac{f_l(\theta_l; t)W_l(t)}{y_t(\neg X_D, C_A, U_0)}$$
$$\phi_{l,B} = \frac{[1 - f_l(\theta_l; t)] W_l(t)}{y_t(\neg X_D, C_B, U_0)}.$$

Note that the vaccination constant is actually not a constant since it depends on time dependent parameters. This is, however, just a naming convention has no further implications for our model.

3.1 Objective function

Given a functional form of f_l, a specific $\bar{\theta}_l \in \mathbb{R}^z$ is called a *strategy* for vaccine l. A *vaccination strategy* $\bar{\Theta} = \begin{pmatrix} \bar{\theta}_1 \\ \bar{\theta}_2 \end{pmatrix}$ is a collection of strategies defined for both vaccines l. We label the strategy Θ_{EU} that assigns the relative population size of country A to be the fraction of vaccines assigned to country A,

$$f_l(\theta_{EU}, t) = \frac{y_0(\neg X_D, C_A)}{y_0(\neg X_D)}, \tag{18}$$

as *current EU strategy* or *current strategy* (European Commission, 2021a). Within the real-world, member states of the EU can refrain from buying their whole quantity and therefore other member states can decide to buy it. We account for this implicitly within our optimization. Since every allocation can be seen as a case where one country waives its right for a certain amount of shots. However, further research could concern incorporating a more game theoretical approach of competing countries.

We denote the number of deceased individuals in country A, conditioned on the current strategy, by $y_T(X_D, C_A; \Theta_{EU})$ and the corresponding number in country B by $y_T(X_D, C_B; \Theta_{EU})$. We use this strategy as baseline case to examine how we can improve using an optimal strategy. An optimal strategy Θ^* is the solution to the minimization problem

$$\begin{aligned}
&\underset{\Theta \in \mathbb{R}^{2z}}{\arg\min} \quad y_T(X_D) \\
&\text{subject to} \quad \phi_{l,A} = \frac{f_l(\theta_l; t) W_l(t)}{y_t(\neg X_D, C_A, U_0)} \quad &&\text{for } l \in \{1, 2\}, &&\text{(C.1)} \\
&\qquad\qquad\quad \phi_{l,B} = \frac{[1 - f_l(\theta_l; t)] W_l(t)}{y_t(\neg X_D, C_B, U_0)} \quad &&\text{for } l \in \{1, 2\}, &&\text{(C.2)} \\
&\qquad\qquad\quad \Theta = \begin{pmatrix} \theta_1' & \theta_2' \end{pmatrix}', &&&&\text{(C.3)} \\
&\qquad\qquad\quad \beta, \eta, \gamma, \delta_{k,l}, \omega_{k,l}, Y(0), W_l(t) &&&&\text{(C.4)}
\end{aligned}$$

and we call it *optimal vaccination strategy* with respect to the given minimization problem. Conditions $C.1$, $C.2$, and $C.3$ indicate how the parameter vector Θ affects the model. $C.4$ specifies that all exogenous parameters are set to a constant value or exogenous function.

If additionally constraints $C.5$ and $C.6$ are satisfied,

$$y_T(X_D, C_A) < y_T(X_D, C_A; \Theta_{EU}) \tag{C.5}$$

$$y_T(X_D, C_B) < y_T(X_D, C_B; \Theta_{EU}) \tag{C.6}$$

the optimal strategy is Pareto optimal and we call it *Pareto optimal vaccination strategy*. The Pareto optimality conditions ensure that both countries have less deceased individuals as within the current strategy. Taking the perspective that both countries can veto against strategies, non Pareto optimal strategies might not be implementable since no country would agree to deviate from the current strategy if it experiences more deceased individuals with the new strategy.

As objective we choose the total number of deceased individuals. Other objectives like the total number of infectious individuals, or some combination of both, could be considered as well. We decided to choose the total number of deaths such that the death protection parameters $\omega_{k,l}$ influence the solution.

3.2 Functional form of the vaccine allocation

We examine two functional forms of f_l. First, f_l is a stepwise function. Second, f_l is a logistically transformed third order spline function. Both forms can be parameterized using the parameter vector θ_l. To define the functional forms, we subdivide the interval $[0, T]$ into a tagged partition $0 = t_0 < t_1 < \cdots < t_z = T$. Let $\mathcal{T}_i = [t_{i-1}, t_i)$, for $i = 1, \ldots, z$, be the corresponding intervals of the tagged partition. We label $\mathcal{T}$ as the *i-th decision period*. To be more precise on the functional form of f_l, we subdivide the parameter vector into its components $\theta_l = \begin{pmatrix} \theta_{l,1} & \theta_{l,2} & \ldots & \theta_{l,z} \end{pmatrix}'$.

Stepwise. In this world, policy makers determine a fraction that is allocated to country A for a fixed decision period $\mathcal{T}_i$, evaluate, and then adjust before the next decision period T_{i+1} begins. In Figure 6 we show an exemplary vaccination strategy for vaccine l.

In mathematical terms, every $\theta_{l,i} \in [0, 1]$ is assigned to an interval $\mathcal{T}_i$. The parameters $\theta_{l,i}$ are in this case the fractions of vaccines assigned to country A.

$$f_l(\theta_l; t) = \theta_{l,i} \quad \forall t \in \mathcal{T}_i. \tag{20}$$

Note that the current EU strategy is a special case of a step function that has $\theta_{l;1} = \theta_{l,2} = \ldots = \theta_{l,z} = y_0(\neg X_D, C_l)/y_0(\neg X_D)$, assuming that the allocations are not adjusted for changes in the population sizes over the course of the pandemic.

Splines. In this world, policy makers decide on the start and end values of the vaccine allocations within each interval $\mathcal{T}_i$. Given the boundary values, one polynomial for each interval $\mathcal{T}_i$ is computed, and logistically transformed to meet the unit interval domain of the fractions. By using polynomials, rather than constant functions, we allow for more complex
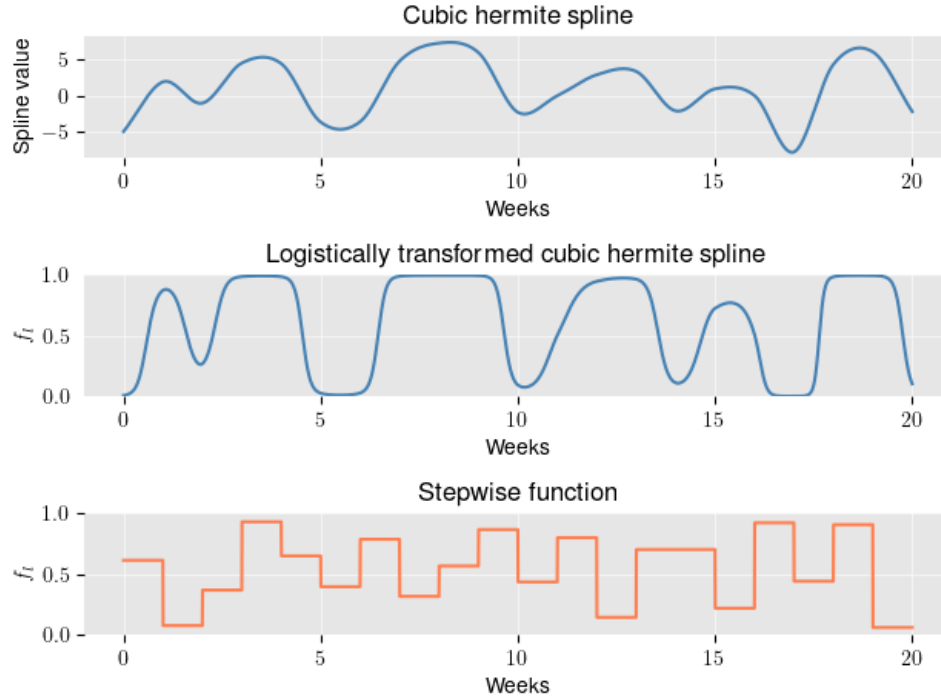
Note: Examples of a piecewise vaccine allocation in orange and a spline allocation in blue. The first graph depicts the values of the spline and the second graph shows the corresponding transformed function that maps the values into the unit interval. The third graph shows a different approach using a piecewise constant function. Decision intervals have a duration of 2 weeks.

Figure 6: Exemplary vaccination strategies.

policy decisions within one decision period $\mathcal{T}_i$ since fluctuations within one decision period can be taken into account. However, one should note that this exercise is rather theoretical and aims to show what strategies could be achieved theoretically.

We use splines instead of a global polynomial interpolation since they are practical with respect to construction and global interpolations might suffer from undesired properties, as in Runge's phenomenon (Runge, 1901).

Figure 6 shows an exemplary spline and how it is shrinked via the logistic function $\sigma(x)$ into the unit interval, via the logistic function, $\sigma(x)$ to obtain values between zero and one. Given a polynomial from the third order polynomial ring over the real numbers $P_{l,i}(t) \in \mathbb{R}_3(t)$, the fraction is mathematically described by the composition of the polynomial and the logistic function

$$f_l(\theta; t) = \frac{1}{1 + \exp\left(-P_{l,i}(t)\right)} \quad \forall t \in \mathcal{T}_i. \tag{21}$$

We chose $P_{l,i}(t)$ to be in cubic hermite form. The name cubic arises from the condition that every $P_{l,i}(t)$ is maximal a third-order polynomial. The name hermite indicates that

16

the derivatives at the boundaries $P'_{l,i}(t_{i-1})$ are computed using finite differences. We use central finite differences and forward as well as backward finite differences at the respective boundaries t_0 and t_z

$$P'_{l,1}(t_0) \approx \frac{P_{l,1}(t_1) - P_{l,1}(t_0)}{t_1 - t_0} \tag{22}$$

$$P'_{l,i}(t_{i-1}) \approx \frac{1}{2} \left[\frac{P_{l,i}(t_i) - P_{l,i}(t_{i-1})}{t_i - t_{i-1}} + \frac{P_{l,i-1}(t_{i-1}) - P_{l,i-1}(t_{i-2})}{t_{i-1} - t_{i-2}} \right]$$

$$P'_{l,z}(t_z) \approx \frac{P_{l,z}(t_z) - P_{l,z}(t_{z-1})}{t_z - t_{z-1}}$$

.

If we have the two functional values at the boundaries and approximations for their derivatives, we have four conditions to specify the polynomial of order three. Thus, we can parameterize the splines by specifying the polynomial values at the boundaries

$$P_{l,i}(t_{i-1}) = \theta_{l,i-1} \tag{23}$$

$$P_{l,i}(t_i) = \theta_{l,i}$$

The polynomial $P_{l,i}(t)$ is given as a linear combination of four basis polynomials $B_1(t), B_2(t), B_3(t), B_4(t) \in \mathbb{R}_3(t)$ with the boundary values of the polynomial and its derivative. Let $t' = (t - t_{i-1})/(t_i - t_{i-1})$ for $t \in \mathcal{T}_i$ and

$$P_{l,i}(t) = B_1(t') \overbrace{P_{l,i}(t_{i-1})}^{\theta_{l,i-1}} + B_2(t')(t_i - t_{i-1})P'_{l,i}(t_{i-1}) \tag{24}$$

$$+ B_3(t') \underbrace{P_{l,i}(t_i)}_{\theta_{l,i}} + B_4(t')(t_i - t_{i-1})P'_{l,i}(t_i) \quad \forall t \in \mathcal{T}_i.$$

The scalars of the linear combination are dependent on the parameter vector θ_l through (22) and (23). The basis polynomials are defined by $B_1(t) = 2t^3 - 3t^2 + 1, B_2(t) = t^3 - 2t^2 + t, B_3(t) = -2t^3 + 3t^2$ and $B_4(t) = t^3 - t^2$. Note that the imposed structure of $P_{l,i}(t)$ is well-defined, which can be verified by evaluating the polynomial and its derivative at the boundaries t_{i-1} and t_i. We provide the calculations in the appendix A.1.2.

We show that the basis polynomials indeed form a basis of $\mathbb{R}_3(t)$. Showing the basis property proves that the four polynomials span $\mathbb{R}_3(t)$ and we therefore do not exclude any polynomials from the space of policies that could be implemented.

Theorem 1. $B_1(t), B_2(t), B_3(t), B_4(t) \in \mathbb{R}_3(t)$ *form a polynomial basis of* $\mathbb{R}_3(t)$.

Proof. The proof is moved to the Appendix A.1.3. $\qquad\square$

4 Stochastic model

Within the deterministic model, we have assumed that for each reaction R_j, the number of times the reaction happens within one unit of time is deterministic, see Equation (2). However, it is more likely the reactions occur random over time. To account for this, we test our deterministically derived optimal vaccination strategy and test it in a stochastic set-up, where the number of times reaction R_j happens, is a random variable.

τ-**leaping**. We impose an arbitrary order to all subcompartments. We do so by using n features $F_1, \ldots F_n$, such that $\cup_{i=1}^{n} \mathcal{C}_t(F_i) = \mathcal{C}_t()$ and $\mathcal{C}_t(F_1), \ldots, \mathcal{C}_t(F_n)$ are mutually disjoint. We specify the state of the system in terms of the subcompartments $Y(t) = \begin{pmatrix} y_t(F_1) & y_t(F_2) & \ldots & y_t(F_n) \end{pmatrix}'$. Recall that $\mathbf{S} \in \mathbb{R}^{n \times m}$ is the stoichiometric matrix, as defined in (5), with coefficients s_{ij} and columns $s_{.j}$. R_j, for $j = 1, \ldots, m$, is the j-th reaction. Let $V_{t,j}$ be the random variable counting the number of times R_j will fire within the interval $[t, t+\tau)$, for $\tau \in \mathbb{R}_+$. We denote by V_t the random vector collecting the random variables $V_{t,1}, \ldots, V_{t,m}$. Dividing the whole period of interest $[0, T]$ in intervals of length τ, the leaping is an iterative update of the discretizised system's state

$$Y(t+\tau) = Y(t) + \mathbf{S}V_t. \tag{25}$$

This equation is the quivalent to equation (3), with the only difference that the number of reactions within a given interval is random in Equation (25).

The change in the system's state $\Delta Y(t) = Y(t+\tau) - Y(t) = \mathbf{S}V_t$ can be written in terms of a linear combination of the columns of $\mathbf{S}$ with random scalars $K_{t,j}$

$$\Delta Y(t) = \sum_{j=1}^{m} K_{t,j} \cdot s_{.j}. \tag{26}$$

$s_{.j}$ consists of the stoichiometry for each compartment i according to reaction R_j and therefore indicates how the state of the system changes if reaction R_j happens. $K_{t,j}$ is the number of occurences of reaction R_j. Thus, the product is the system's change due to R_j. Aggregating over all reactions yields the total change of the system R_j, similar to the deterministic equation (3).

So far we have not specified the distribution of K_t. We are interested in the conditional joint probability distribution $\mathbb{P}_t(K_{t,1} = k_{t,1}, \ldots, K_{t,m} = k_{t,m}|\tau)$ of the random vector $K_t = \begin{pmatrix} K_{t,1}, \ldots, K_{t,m} \end{pmatrix}'$ conditioned on the state of the system and a fixed interval size. Recall that we have defined $\mathbb{P}_t$ to be the conditional probability with respect to the state of

the system and we therefore omit to write the condition explicitly within as condition statement. Assuming independence of all $K_{t,1}, \ldots, K_{t,m}$, we simplify the problem to specifying the marginal distributions. Let $a_j(y)$ be the propensity function $\mathbb{P}_t(K_{t,j} = 1 | \tau = 1)$ of the j-th reaction with respect to the state of the system $Y(t) = y$. We assume that for infinitesimal small dt

$$\mathbb{P}_t(K_{t,j} = 1 | \tau = dt) = a_j(y) \cdot dt, \tag{27}$$

is the probability that R_j fires once within the interval $[t, t + dt)$ and $(K_{t,j} | Y(t), \tau = dt)$ is Bernoulli $\text{Ber}(a_j(y) \cdot dt)$ distributed. The Bernoulli assumption is justified by choosing dt infinitesimal small, such that R_j fires at most once almost surely.

For simplicitly we assume that $\frac{\tau}{dt}$ is an integer. If we assume that $a_j(y)$ is constant within $[t, t + \tau)$, we can partition the interval in $\frac{\tau}{dt}$ subintervals with length dt. In each of these subintervals the conditional random variable is Bernoulli distributed $(K_{t+s \cdot dt,j} | Y(t), \tau = dt) \sim \text{Ber}(a_j(y) \cdot dt)$ for $s = 0, 1, \ldots, \frac{\tau}{dt} - 1$. Thus, the sum

$$\sum_{s=0}^{\frac{\tau}{dt}-1} (K_{t+s \cdot dt,j} | Y(t), \tau = dt) \sim \text{B}\left(\frac{\tau}{dt}, a_j(y) \cdot dt\right) \tag{28}$$

follows a binomial distribution. The practical problem of this Binomial distribution is that sampling from it requires to define a value for dt. By definition dt is infinitesimal small, such that we actually aim for $dt \to 0$. Fortunately, $dt \to 0$ leads to a Poisson random variable that can be specified by the known τ and $a_j(y)$.

Theorem 2. $B\left(\frac{\tau}{dt}, a_j(y) \cdot dt\right) \xrightarrow{d} Po(a_j(y) \cdot \tau)$ if $dt \to 0$.

Proof. The proof is moved to the Appendix A.1.4 □

The τ- leaping algorithm we use is the stochastic Euler algorithm with fixed step-size. We use a fixed step-size since we have a predefined step-size within the deterministic model and to test the deterministically derived vaccination strategies properly, we decided to use the same step-size for the stochastic model. The algorithm requires the initialization of the system $Y(0)$ and specifying the stoichiometry. Within the update steps, it mainly exploits Equation (25).

Algorithm 1: Stochastic Euler algorithm

   Result: $Y(t) \quad \forall t \in [0, T]$

   Initialize $Y(0) = Y_0, t = 0$, and set fixed $\tau, \mathbf{S}$;

   while $t < T$ **do**

      | Set y = Y(t);

      | Draw $K_{t,j} \sim \mathrm{Po}(a_j(y)\tau)$ for all $j = 1, \ldots, m$;

      | Compute $Y(t + \tau) = Y(t) + \mathbf{S}K_t$;

      | Store $Y(t + \tau)$;

      | Update $a_j = a_j(Y(t + \tau))$ for all $j = 1, \ldots, m$;

      | Update $t = t + \tau$;

   end
---

5 Simulation and optimization

We use values derived from the literature to calibrate our models fixed parameters. We simulate one model using a stepwise vaccination strategy and one model using s spline vaccination strategy.

5.1 Calibration

Vaccine parameter. Within our model there exist two vaccines U_1 and U_2. Whereas in the EU, as of July 2021, 4 vaccines are approved and two are in the development phase (European Commission, 2021b). To establish the link from our theoretical model to the real-world COVID-19 vaccines, we use data based on the four approved vaccines to calibrate our model. Vaccine U_1 represents the messenger ribonucleic acid (mRNA) vaccines and vaccine U_2 represent the vector vaccines. In contrast to conventional vaccines, mRNA vaccines do not contain viral proteins themselves. They only contain the information human cells need to produce a virus trait that triggers the desired immune response (Biontech, 2021). This new method has shown a significant improvement with regard to immunity. See Table 2.

Currently approved mRNA vaccines are Comirnaty, also known as BNT162b2, from Pfizer-BioNTech and Spikevax, also known as mRNA-1273, from Moderna. The approved vector vaccines are Vaxzevria from Oxford-Astra Zeneca and Janssen, also known as Johnson & Johnson COVID-19 vaccine, from Janssen Vaccines.

We use efficacy values reported within the literature to calibrate the vaccine specific parameters $\delta_{k,l}$ and $\omega_{k,l}$. Efficacy describes the effect with respect to perfect conditions

whereas effectiveness measures the effect under real-world clinical settings (Gartlehner et al., 2006). Therefore, real-world effectiveness could be lower than the numbers reported in Table 2. We use data from the early alpha virus type to calibrate the wild type parameters and data from the lately spreading delta variant to calibrate the mutant parameters.   Due to

Vaccine	Efficacy		Sources
	alpha	delta	
Comirnaty	94%-95%	87%-95%	Callaway (2021), Nasreen et al. (2021), Polack et al. (2020), Prüβ (2021), Sheikh et al. (2021)
Spikevax	94%	-	Oliver (2021b), Prüβ (2021)
Vaxzevria	66%-73%	60%-71%	Callaway (2021), Emary et al. (2021), Prüβ (2021), Stowe et al. (2021)
Janssen	66%	-	Oliver (2021a), Sadoff et al. (2021)

Note: Efficacy is measured as protection against an infection after 14 days of the second vaccine shot.

Table 2: Vaccine efficacy

the recent spread of the delta variant, data is still limited and we did not find reliable sources for the delta efficacy of Spikevax and Janssen. For the latter a recent study of Jongeneelen et al. (2021) reports that, even though real world effectiveness has been shown, they found no efficacy for the Janssen vaccine against the delta variant. Since their study only included 8 individuals and we therefore refrain from using the study to calibrate our model.

With respect to Table 2, we decided to set the protection of the mRNA vaccines against an infection with the wild type (alpha variant) to be $\delta_{1,W} = 0.94$ and against an infection with the mutant (delta variant) to be $\delta_{1,M} = 0.9$. For the vector vaccines we chose for the wild type $\delta_{2,W} = 0.7$ and for the mutant $\delta_{2,M} = 0.65$.

Abu-Raddad et al. (2021) report Comirnaty to protect from hospitalization by 97.4%. Tenforde (2021) find that Comirnaty and Spikevax yield 94% protection against hospitalization within the the age group of ≥ 65 aged individuals. Voysey et al. (2021) report a 100% efficacy against hospitalization regarding Vaxzevria and the alpha variant. We generalize the empirical results and set the value against death protection $\omega_{k,l} = 0.99$ for all $k \in \{W, M\}$ and $l \in \{1, 2\}$.

Harris et al. (2021) found that in a study of more than 365,000 British households, mixed with vaccinated and unvaccinated individuals, that full vaccination with Comirnaty or Vaxzevria reduces the transmission probability by 40%-60%. We therefore set $\delta = 0.5$.

Basic reproduction number. The basic reproduction number R_l of virus type l is the

average number of individuals infected by one infectious individual. Translated to our model, this yields the following equations

$$R_W = \frac{\beta}{\lambda} \tag{29}$$
$$R_M = \frac{\eta\beta}{\lambda},$$

Recall that $1/\lambda$ is the average time an individual is infected and β, or $\eta\beta$, is the average number of individuals infected by one infectious individual per day. The German Robert Koch Institut (2021) reports the basic reproduction number to be between 2.8 and 3.8. Moreover, they state that an individual is around 10 days infectious. We use $\lambda = 0.1$, $R_W = 3$ and $R_M = 3.6$, yielding $\beta = 0.3$ and $\eta = 1.2$. Note that this numbers do not take non-pharmaceutical measures, like testing and social distancing, into account and therefore our pandemic might have higher death numbers an be comparatively fast.

Death rate. Baud et al. (2020) find a death rate of 5.7% for symptomatic cases. However, this number might be overestimated due to undetected asymptomatic cases. Wu and McGoogan (2020) account for asymptomatic cases and find estimates to be between 2%-3%. We therefore use $p = 2.5\%$ for our simulations.

Start conditions. We set the initial population size of susceptible individuals in both countries to $y_0(X_S, C_A) = y_0(X_S, C_B) = 80$ million, a country size similar to Germany. Country A starts with one wild type infectious individual $y_0(X_I, C_A, V_W) = 10$ and country B with one mutant type infected individual $y_0(X_I, C_B, V_M) = 10$. All other compartments are set to zero at $t = 0$.

Distance. To specify the cross-border meeting modifier $b(d(A, B))$, we use tourism data from Germany and France. We use France since it is populationwise the largest country with a border to Germany. In 2016, $1,725,854$ individuals from France traveled to Germany and stayed on average for two days (Statistisches Bundesamt, 2017). We divide this number by 366 to get an estimate of the average number of French individuals in Germany at each day in 2016 and scale it by $\frac{80}{67}$ to adjust that our second country has a population size of 80 million but France has around 67 million inhabitants $\frac{2 \cdot 1,725,854}{366} \cdot \frac{80}{67} \approx 11,261$. Assuming that the same number of French individuals have been in Germany every day and using equation (33) with a constant proportion $y_t(\neg X_D, C_B)/y_t(\neg X_D)$ yields

$$b(d(A, B)) = \frac{11,261}{80,000,000} \approx 0.0002$$

Note that this estimate is rather conservative since we do not take commuters and unregistered visits, such as shopping trips, into account.

Length of decision periods. We set the length of the whole decision period to $T = 140$ and subdivide the length of each decision interval $\mathcal{T}_i$ to 14 days.

Vaccine inflow. The daily vaccine inflow $W_l(t)$ is computed using EU data of the vaccine inflow taken from the open source data bank of the European Centre for Disease Prevention and Control (2021). The data reports the weekly inflow of vaccines for all countries within the EU. We accumulate the numbers of Corminarty and Spikevax to compute the total numbers of mRNA vaccines and accumulate the total numbers of Vaxzevria and Janssen to compute the total numbers of vector vaccines per week. We scale this number down to our model's population size by dividing it through the total number of EU habitants and multiplictae it by the number of individuals in our model. We subsequently accumulate the vaccines within each 14-day interval $\mathcal{T}_i$ and divide this number by 14 to get the average number of vaccine doses inflow per vaccine and day. Thus, the inflow per day of each vaccine is constant within each interval $\mathcal{T}_i$ but varies across intervals and vaccines.
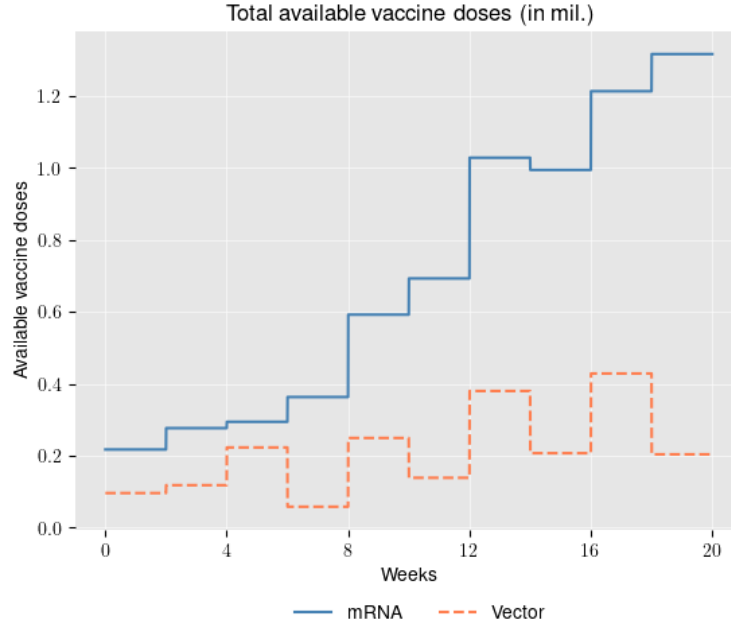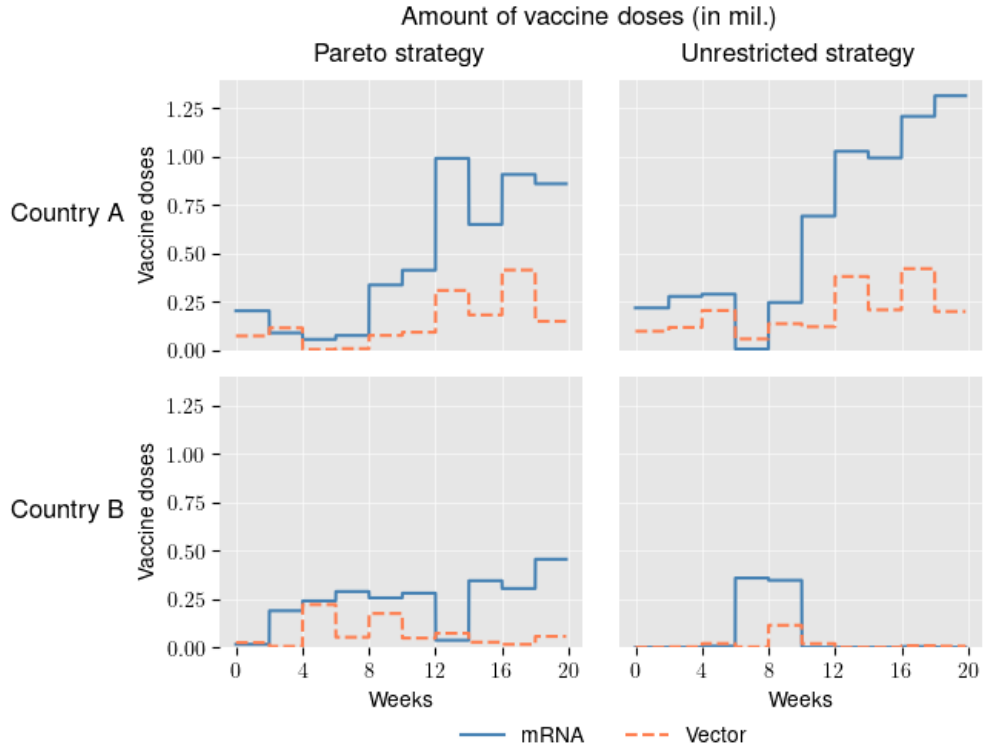

Note:

Figure 7: Vaccines

5.2 Simulations

We use Python and mainly its libraries libSBML (Bornstein et al., 2008) and AMICI (Fröhlich et al., 2021) to implement our models. pyPESTO (Schälte et al., 2021) is our main tool for optimization. To minimize the optimization problem, we use the L-BFGS-B algorithm (Zhu et al., 1997) for which pyPESTO uses Scipy's (Virtanen et al., 2020) implementation. For each optimization we run a muli-start using 50 starts and choose the corresponding vaccination strategy that minimizes the objective. For each start, we draw uncorrelated start parameters $\theta_{l,i} \sim \mathcal{U}(0,1)$. In the case of Pareto optimal constraints, we only accept a starting vector Θ if the Pareto constraints $C.7$ and $C.8$ are satisfied. Otherwise we reject it and draw a new sample until 50 starts are reached.

optimal results splines fractions in appendix
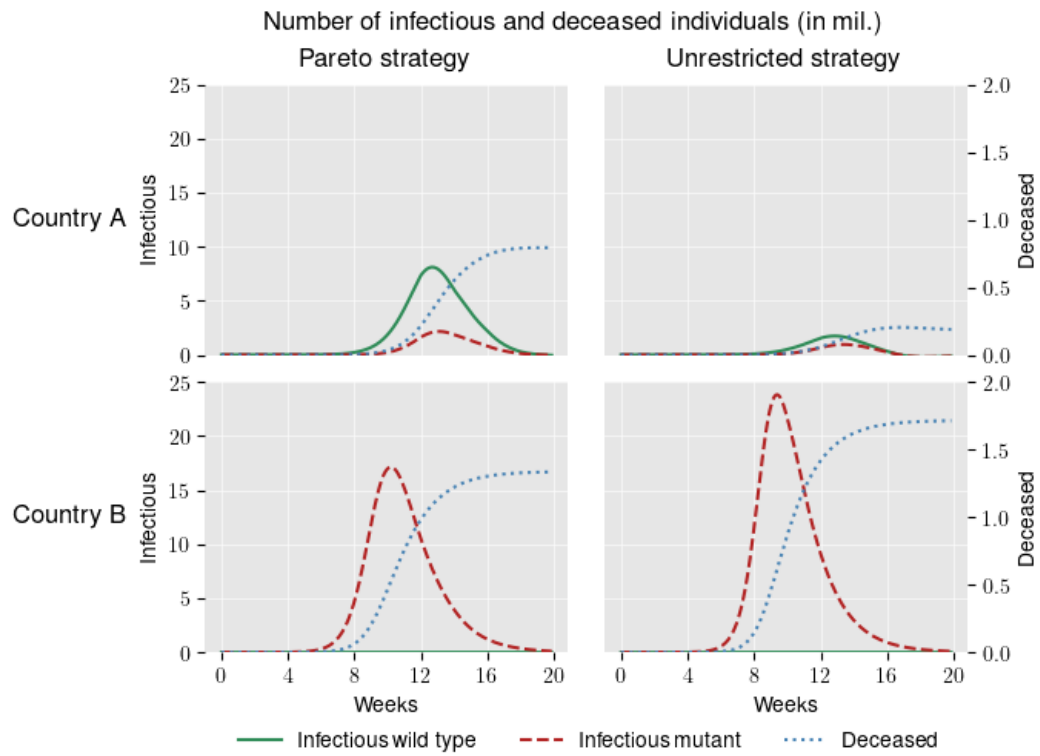

Note:

Figure 8: Vaccines

same for infectious individuals

waterfall

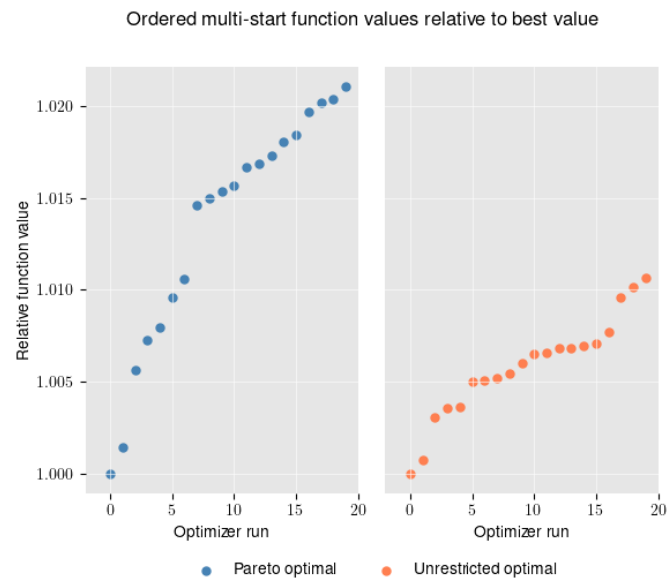same for unrestricted waterfall plots for both; 4 best strategies for both

table comparing three variants (see orchestra presentation)

**optimal results splines** fractions in appendix

Figure 9: Vaccines

Figure 10: Vaccines

	Strategies		
	Current	Pareto optimal	Unrestricted optimal
Comirnaty	94%-95%	87%-95%	Callaway (2021), Nasreen et al. (2021), Polack et al. (2020), Prüβ (2021), Sheikh et al. (2021)
Spikevax	94%	-	Oliver (2021b), Prüβ (2021)
Vaxzevria	66%-73%	60%-71%	Callaway (2021), Emary et al. (2021), Prüβ (2021), Stowe et al. (2021)
Janssen	66%	-	Oliver (2021a), Sadoff et al. (2021)

Note:

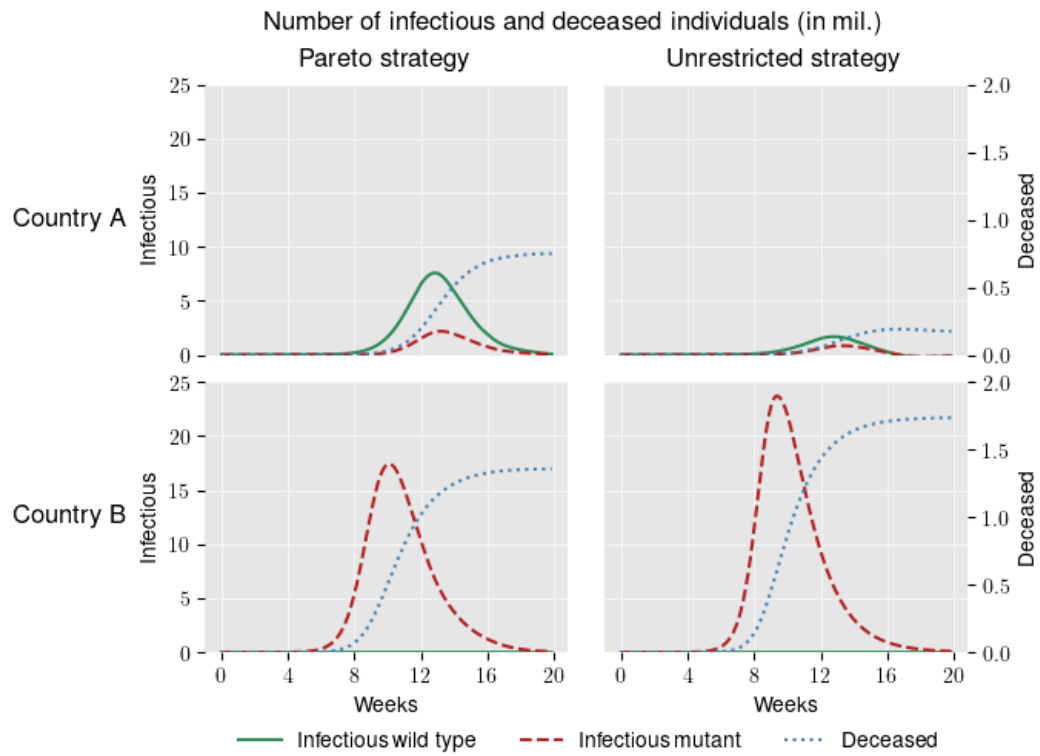Table 3: Number of deceased individuals depending on the vaccination strategy.
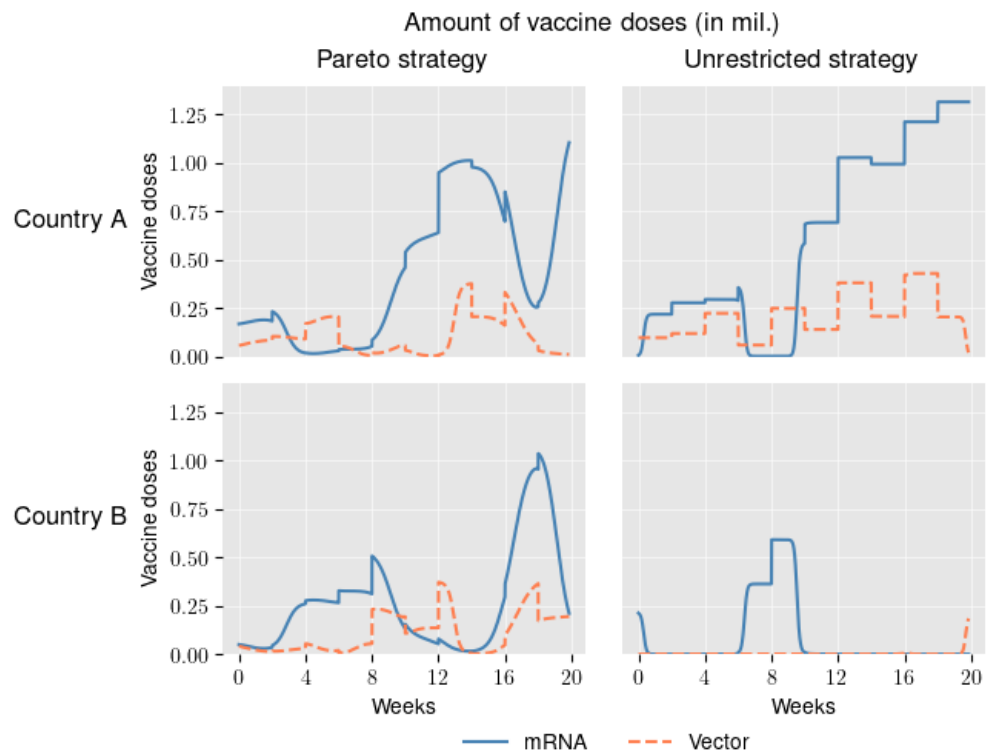
Note:
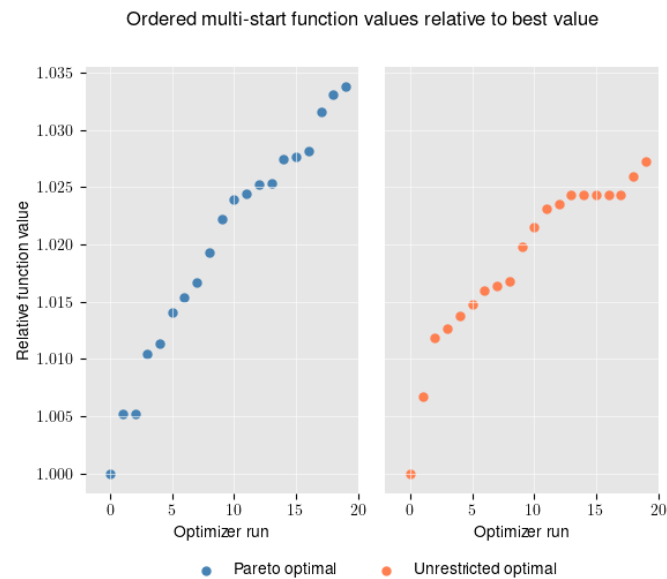
Figure 11: Vaccines

same for infectious individuals

waterfall

table comparing three variants (see orchestra presentation);

Number of infectious and deceased individuals (in mil.)

Figure 12: Vaccines

Ordered multi-start function values relative to best value

Note:

Figure 13: Vaccines

5.2.1 Test with stochastic set-up

6 Sensitivity analysis

References

Abu-Raddad, L. J., Chemaitelly, H., and Butt, A. A. (2021). Effectiveness of the BNT162b2 Covid-19 vaccine against the B.1.1.7 and B.1.3.51 variants. *New England Journal of Medicine.*

Baud, D., Qi, X., Nielsen-Saines, K., Musso, D., Pomar, L., and Favre, G. (2020). Real estimates of mortality following COVID-19 infection. *The Lancet*, 20(7):773.

Biontech (2021). mRNA vaccines to address the COVID-19 pandemic. `https://biontech.de/covid-19-portal/mrna-vaccines`, Last accessed on 2021-07-12.

Bornstein, B. J., Keating, S. M., Jouraku, A., and Hucka, M. (2008). LibSBML: An API library for SBML. *Bioinformatics*, 24(6):880–881.

Byambasuren, O., Cardona, M., Bell, K., Clark, J., McLaws, M.-L., and Glasziou, P. (2020). Estimating the extent of asymptomatic COVID-19 and its potential for community transmission: Systematic review and meta-analysis. *Official Journal of the Association of Medical Microbiology and Infectious Disease Canada*, 5(4):223–234.

Callaway, E. (2021). Delta coronavirus variant: Scientists brace for impact. *Nature*, 595:17–18.

Centers for Disease Control and Prevention (2021). Key things to know about COVID-19 vaccines. `https://www.cdc.gov/coronavirus/2019-ncov/vaccines/keythingstoknow.html`, Last accessed on 2021-07-12.

Davies, N. G., Jarvis, C. I., Edmunds, W. J., Jewell, N. P., Diaz-Ordaz, K., and Keogh, R. H. (2021). Increased mortality in community-tested cases of SARS-CoV-2 lineage B.1.1.7. *Nature*, 593(7858):270–274.

Emary, K. R. W., Golubchik, T., Aley, P. K., Ariani, C. V., et al. (2021). Efficacy of chadox1 nCoV-19 (azd1222) vaccine against SARS-CoV-2 variant of concern. *The Lancet*, 397(10282):1351–1362.

European Centre for Disease Prevention and Control (2021). Data on COVID-19 vaccination in the EU/EEA. `"https://opendata.ecdc.europa.eu/covid19/vaccine_tracker/xlsx/data.xlsx"`, Last accessed on 2021-07-12.

European Commission (2021a). Questions and answers on COVID-19 vaccination in the EU. `https://ec.europa.eu/info/live-work-travel-eu/coronavirus-response/safe-covid-19-vaccines-europeans/questions-and-answers-covid-19-vaccination-eu_en`, Last accessed on 2021-07-13.

European Commission (2021b). Safe COVID-19 vaccines for Europeans. "https://ec.europa.eu/info/live-work-travel-eu/coronavirus-response/safe-covid-19-vaccines-europeans_en", Last accessed on 2021-07-13.

Fröhlich, F., Weindl, D., Schälte, Y., Pathirana, D., Paszkowski, Ł., Lines, G. T., Stapor, P., and Hasenauer, J. (2021). AMICI: High-performance sensitivity analysis for large ordinary differential equation models. *Bioinformatics*. btab227.

Gartlehner, G., Hansen, R. A., Nissman, D., Lohr, K. N., and Carey, T. S. (2006). *Criteria for distinguishing effectiveness from efficacy trials in systematic reviews*. Agency for Healthcare Research and Quality, Rockville, MD.

Gillespie, D. T. (1977). Exact stochastic simulation of coupled chemical reactions. *The Journal of Physical Chemistry*, 81(25):2340–2361.

Gillespie, D. T. (2001). Approximate accelerated stochastic simulation of chemically reacting systems. *The Journal of Chemical Physics*, 115(4):1716–1733.

Harris, R. J., Hall, J. A., Zaidi, A., Andrews, N. J., Dunbar, J. K., and Dabrera, G. (2021). Impact of vaccination on household transmission of SARS-COV-2 in England. *medRxiv*.

Jongeneelen, M., Kaszas, K., Veldman, D., Huizingh, J., van der Vlugt, R., Schouten, T., Zuijdgeest, D., Uil, T., van Roey, G., Guimera, N., et al. (2021). Ad26. COV2. S elicited neutralizing activity against delta and other SARS-CoV-2 variants of concern. *bioRxiv*.

Nasreen, S., He, S., Chung, H., Brown, K. A., Gubbay, J. B., Buchan, S. A., Wilson, S. E., Sundaram, M. E., Fell, D. B., Chen, B., et al. (2021). Effectiveness of COVID-19 vaccines against variants of concern, Canada. *medRxiv*.

Oliver, S. E. (2021a). The advisory committee on immunization practices' interim recommendation for use of Janssen COVID-19 vaccine. *Morbidity and Mortality Weekly Report*, 70(9):329–332.

Oliver, S. E. (2021b). The advisory committee on immunization practices' interim recommendation for use of Moderna COVID-19 vaccine. *Morbidity and Mortality Weekly Report*, 69(5152):1653–1656.

Poisson, S. D. (1835). Recherches sur la probabilité des jugements, principalement en matiére criminelle. *Comptes-Rendus Hebdomadaires des Séances de l'Académie des Sciences*, 1:473–494.

Polack, F. P., Thomas, S. J., Kitchin, N., Absalon, J., Gurtman, A., Lockhart, S., Perez, J. L., Marc, G. P., Moreira, E. D., Zerbini, C., et al. (2020). Safety and efficacy of the BNT162b2 mRNA Covid-19 vaccine. *New England Journal of Medicine*.

Prüβ, B. M. (2021). Current state of the first COVID-19 vaccines. *Vaccines*, 9(1):30.

Robert Koch Institut (2021). Epidemiologischer Steckbrief zu SARS-CoV-2 und COVID-19. `https://www.rki.de/DE/Content/InfAZ/N/Neuartiges_Coronavirus/Steckbrief.`, Last accessed on 2021-07-12.

Roy, S. (2020). COVID-19 reinfection: Myth or truth? *SN Comprehensive Clinical Medicine*, 2(6):710–713.

Runge, C. (1901). Über empirische funktionen und die interpolation zwischen äquidistanten ordinaten. *Zeitschrift für Mathematik und Physik*, 46(224-243):20.

Sadoff, J., Gray, G., Vandebosch, A., Cárdenas, V., Shukarev, G., Grinsztejn, B., Goepfert, P. A., Truyers, C., Fennema, H., Spiessens, B., et al. (2021). Safety and efficacy of single-dose Ad26. COV2. S vaccine against COVID-19. *New England Journal of Medicine*, 384(23):2187–2201.

Schälte, Y., Vanhoefer, J., Fröhlich, F., and Stapor, P. (2021). pyPESTO - Parameter estimation toolbox for python.

Sheikh, A., McMenamin, J., Taylor, B., and Robertson, C. (2021). SARS-CoV-2 Delta VOC in Scotland: Demographics, risk of hospital admission, and vaccine effectiveness. *The Lancet*, 397(10293):2461–2462.

Skelly, D. T., Harding, A. C., Gilbert-Jaramillo, J., Knight, M. L., Longet, S., Brown, A., Adele, S., Adland, E., Brown, H., Team, M. L., et al. (2021). Vaccine-induced immunity provides more robust heterotypic immunity than natural infection to emerging SARS-CoV-2 variants of concern. *Research Square preprint*.

Statistisches Bundesamt (2017). Ergebnisse der Monatserhebung im Tourismus.

Stowe, J., Andrews, N., Gower, C., Gallagher, E., Utsi, L., and Simmons, R. (2021). Effectiveness of COVID-19 vaccines against hospital admission with the Delta (B. 1.617. 2) variant. *Public Health England*.

Tenforde, M. W. (2021). Effectiveness of Pfizer-BioNTech and Moderna vaccines against COVID-19 among hospitalized adults aged $\geq$ 65 years. *Morbidity and mortality weekly report*, 70(18):674–679.

Virtanen, P., Gommers, R., Oliphant, T. E., Haberland, M., Reddy, T., Cournapeau, D., Burovski, E., Peterson, P., Weckesser, W., Bright, J., van der Walt, S. J., et al. (2020). SciPy 1.0: Fundamental algorithms for scientific computing in python. *Nature Methods*, 17:261–272.

Voysey, M., Clemens, S. A. C., Madhi, S. A., Weckx, L. Y., Folegatti, P. M., Aley, P. K., Angus, B., Baillie, V. L., Barnabas, S. L., Bhorat, Q. E., et al. (2021). Single-dose administration and the influence of the timing of the booster dose on immunogenicity and efficacy of ChAdOx1 nCoV-19 (AZD1222) vaccine: A pooled analysis of four randomised trials. *The Lancet*, 397(10277):881–891.

Wu, Z. and McGoogan, J. M. (2020). Characteristics of and important lessons from the coronavirus disease 2019 (COVID-19) outbreak in China: Summary of a report of 72,314 cases from the Chinese Center for Disease Control and Prevention. *Jama*, 323(13):1239–1242.

Zhu, C., Byrd, R. H., Lu, P., and Nocedal, J. (1997). Algorithm 778: L-BFGS-B: Fortran subroutines for large-scale bound-constrained optimization. *ACM Transactions on Mathematical Software*, 23(4):550–560.

A Appendix

A.1 Calculations and proofs

A.1.1 Meeting probabilities

Using Bayes formula, we can rewrite the conditional probability as follows

$$
\begin{aligned}
\mathbb{P}_t(i_2 \in \mathcal{C}_t(X_S, C_j, F_2) | i_1 \in \mathcal{C}_t(\neg X_D, C_A)) &= \mathbb{P}_t(i_2 \in \mathcal{C}_t(\neg X_D, C_j, F_2) | i_1 \in \mathcal{C}_t(\neg X_D, C_A)) \quad (30) \\
&\cdot \mathbb{P}_t(i_2 \in \mathcal{C}_t(X_S) | i_1 \in \mathcal{C}_t(\neg X_D, C_A), i_2 \in \mathcal{C}_t(\neg X_D, C_j, F_2)) \\
&= \mathbb{P}_t(i_2 \in \mathcal{C}_t(\neg X_D, C_j, F_2) | i_1 \in \mathcal{C}_t(\neg X_D, C_A)) \\
&\cdot \mathbb{P}_t(i_2 \in \mathcal{C}_t(X_S) | i_2 \in \mathcal{C}_t(\neg X_D, C_j, F_2))
\end{aligned}
$$

We use the relative number of susceptible individuals $\mathcal{C}_t(X_S, C_j, F_2)$ across all individuals of $\mathcal{C}_t(\neg X_D, C_j, F_2)$ as approximation of the probability at the second line of the right-hand side

$$
\mathbb{P}_t(i_2 \in \mathcal{C}_t(X_S, F_2) | i_2 \in \mathcal{C}_t(\neg X_D, C_j, F_2)) = \frac{y_t(X_S, C_j, F_2)}{y_t(\neg X_D, C_j, F_2)}. \tag{31}
$$

To account for the origin of i_1 within the first line of the right hand-side, we distinguish between the cases where $i_2 \in \mathcal{C}_t(C_A)$ and $i_2 \in \mathcal{C}_t(C_B)$. Assume that $i_2 \in \mathcal{C}_t(X_S, C_B, F_2)$. If there were no spatial effects to influence the cross-border meeting frequency we would use the unconditional probability

$$
\mathbb{P}_t(i_2 \in \mathcal{C}_t(\neg X_D, C_j, F_2)) = \frac{y_t(\neg X_D, C_j, F_2)}{y_t(\neg X_D)}. \tag{32}
$$

To account for the spatial effects, we introduce a penalty function $b : \mathbb{R}_+ \to [0,1]$ that depends on the distances between both countries $d(A, B)$

$$
\mathbb{P}_t(i_2 \in \mathcal{C}_t(\neg X_D, C_B, F_2) | i_1 \in \mathcal{C}_t(\neg X_D, C_A)) = \mathbb{P}_t(i_2 \in \mathcal{C}_t(\neg X_D, C_B, F_2)) \cdot b(d(A, B)), \tag{33}
$$

Yielding

$$
\mathbb{P}_t(i_2 \in \mathcal{C}_t(X_S, C_B, F_2) | i_1 \in \mathcal{C}_t(\neg X_D, C_A)) = \frac{y_t(X_S, C_j, F_2)}{y_t(\neg X_D)} \cdot b(d(A, B)) \tag{34}
$$

A.1.2 Well-conditioning of Polynomial basis

First note that $B_1(0) = 1$ and $B_2(0), B_3(0), B_4(0) = 0$. Furthermore, $B_1(1), B_2(1), B_4(1) = 0$ and $B_3(1) = 1$. We first compute the function values at the boundaries t_{i-1} and t_i.

$$
\begin{aligned}
P_{l,i}(t_{i-1}) &= B_1(0)P_{l,i}(t_{i-1}) + B_2(0)(t_i - t_{i-1})P'_{l,i}(t_{i-1}) \\
&\quad + B_3(0)P_{l,i}(t_i) + B_4(0)(t_i - t_{i-1})P'_{l,i}(t_i) \\
&= 1 \cdot P_{l,i}(t_{i-1}) + 0 \cdot (t_i - t_{i-1})P'_{l,i}(t_{i-1}) \\
&\quad + 0 \cdot P_{l,i}(t_i) + 0 \cdot (t_i - t_{i-1})P'_{l,i}(t_i) \\
&= P_{l,i}(t_{i-1})
\end{aligned}
$$

$$
\begin{aligned}
P_{l,i}(t_i) &= B_1(1)P_{l,i}(t_{i-1}) + B_2(1)(t_i - t_{i-1})P'_{l,i}(t_{i-1}) \\
&\quad + B_3(1)P_{l,i}(t_i) + B_4(1)(t_i - t_{i-1})P'_{l,i}(t_i) \\
&= 0 \cdot P_{l,i}(t_{i-1}) + 0 \cdot (t_i - t_{i-1})P'_{l,i}(t_{i-1}) \\
&\quad + 1 \cdot P_{l,i}(t_i) + 0 \cdot (t_i - t_{i-1})P'_{l,i}(t_i) \\
&= P_{l,i}(t_i)
\end{aligned}
$$

The derivatives of the basis polynomials are

$$
\begin{aligned}
B'_1(t) &= 6t^2 - 6t \\
B'_2(t) &= 3t^2 - 4t + 1 \\
B'_3(t) &= -6t^2 + 6t \\
B'_4(t) &= 3t^2 - 2t
\end{aligned}
$$

with $B_1(0)' = B_3(0)' = B_4(0)' = 0$ and $B_2(t)' = \frac{1}{t_i - t_{i-1}}$. Moreover, $B'_1(1)' = B_2(1)' = B_3(1)' = 0$ and $B_4(1)' = \frac{1}{t_i - t_{i-1}}$. The derivative of the polynomial is simply

$$
\begin{aligned}
P'_{l,i}(t) &= B'_1(t')P_{l,i}(t_{i-1}) + B'_2(t')(t_i - t_{i-1})P'_{l,i}(t_{i-1}) \\
&\quad + B'_3(t')P_{l,i}(t_i) + B'_4(t')(t_i - t_{i-1})P'_{l,i}(t_i)
\end{aligned}
$$

and therefore

$$
\begin{aligned}
P'_{l,i}(t_{i-1}) &= B'_1(0)P_{l,i}(t_{i-1}) + B'_2(0)(t_i - t_{i-1})P'_{l,i}(t_{i-1}) \\
&\quad + B'_3(0)P_{l,i}(t_i) + B'_4(0)(t_i - t_{i-1})P'_{l,i}(t_i) \\
&= 0 \cdot P_{l,i}(t_{i-1}) + \frac{1}{t_i - t_{i-1}} \cdot (t_i - t_{i-1})P'_{l,i}(t_{i-1}) \\
&\quad + 0 \cdot P_{l,i}(t_i) + 0 \cdot (t_i - t_{i-1})P'_{l,i}(t_i) \\
&= P'_{l,i}(t_{i-1})
\end{aligned}
$$

and

$$
\begin{aligned}
P'_{l,i}(t_{i-1}) &= B'_1(1)P_{l,i}(t_{i-1}) + B'_2(1)(t_i - t_{i-1})P'_{l,i}(t_{i-1}) \\
&\quad + B'_3(1)P_{l,i}(t_i) + B'_4(1)(t_i - t_{i-1})P'_{l,i}(t_i) \\
&= 0 \cdot P_{l,i}(t_{i-1}) + 0 \cdot (t_i - t_{i-1})P'_{l,i}(t_{i-1}) \\
&\quad + 0 \cdot P_{l,i}(t_i) + \frac{1}{t_i - t_{i-1}} \cdot (t_i - t_{i-1})P'_{l,i}(t_i) \\
&= P'_{l,i}(t_i)
\end{aligned}
$$

A.1.3 Polynomial Basis

Theorem 3. $B_1(t), B_2(t), B_3(t), B_4(t) \in \mathbb{R}_3(t)$ *form a polynomial basis of* $\mathbb{R}_3(t)$.

Proof. We need to show that the four polynomials are linearly independent. We do so by writing the polynomials in vector form, collect them in a matrix and show that this matrix has full rank.

$$
\begin{pmatrix}
2 & 1 & -2 & 1 \\
-3 & -2 & 3 & -1 \\
0 & 1 & 0 & 0 \\
1 & 0 & 0 & 0
\end{pmatrix}
\Leftrightarrow
\begin{pmatrix}
0 & 0 & -2 & 1 \\
0 & 0 & 1 & -1 \\
0 & 1 & 0 & 0 \\
1 & 0 & 0 & 0
\end{pmatrix}
\Leftrightarrow
\begin{pmatrix}
0 & 0 & 0 & -1 \\
0 & 0 & 1 & -1 \\
0 & 1 & 0 & 0 \\
1 & 0 & 0 & 0
\end{pmatrix}
\Leftrightarrow
\begin{pmatrix}
0 & 0 & 0 & 1 \\
0 & 0 & 1 & 0 \\
0 & 1 & 0 & 0 \\
1 & 0 & 0 & 0
\end{pmatrix}
$$

Since $B_1(t), B_2(t), B_3(t), B_4(t)$ are four linearly independent polynomials of degree 3, they form a basis of $\mathbb{R}_3(t)$. $\qquad\square$

A.1.4 Convergence in distribution

Theorem 4. $B\left(\frac{\tau}{dt}, a_j(y) \cdot dt\right) \xrightarrow{d} Po(a_j(y) \cdot \tau)$ *if* $dt \to 0$.

Proof. Let p_n be a sequence with $\lim_{n\to\infty} p_n = 0$. We first show that if $\lambda' = n \cdot p_n$ is constant, $n \to \infty$ and $p_n \to 0$, a general Binomial random variable $B(n, p_n)$ converges in distribution

to a Poisson random variable $Po(\lambda')$. Note that this proof is in essence just a restatement of the Poisson limit theorem of Poisson (1835).

$$
\begin{aligned}
\lim_{n\to\infty} \binom{n'}{k} p_n^k (1-p_n)^{n-k} &= \lim_{n\to\infty} \frac{n \cdot (n-1) \cdot \ldots \cdot (n-k+1)}{k!} \left(\frac{\lambda'}{n}\right)^k \left(1-\frac{\lambda'}{n}\right)^{n-k} \\
&= \lim_{n\to\infty} \frac{n^k + O(n^{k-1})}{k!} \left(\frac{\lambda'}{n}\right)^k \left(1-\frac{\lambda'}{n}\right)^{n-k} \\
&= \frac{(\lambda')^k}{k!} \exp(-\lambda')
\end{aligned}
$$

Note that by definition τ is fixed and by assumption $a_i(y)$ is constant within $[t, t+\tau)$. Thus, $\lim_{dt\to 0} \frac{\tau}{dt} = \infty$, $\lim_{dt\to 0} a_i(y) \cdot dt = 0$ and $\frac{\tau}{dt} \cdot a_i(y) \cdot dt = \tau \cdot a_i(y)$. Using the convergence property mentioned above yields the result. $\qquad\square$